

# Thermal properties of electrodeposited bismuth telluride nanowires embedded in amorphous alumina

D.-A. Borca-Tasciuc

*Department of Mechanical and Aerospace Engineering, University of California, Los Angeles, California 90095*

G. Chen<sup>a)</sup>

*Department of Mechanical Engineering, Massachusetts Institute of Technology, Cambridge, Massachusetts 02139*

A. Prieto,<sup>b)</sup> M. S. Martín-González,<sup>c)</sup> and A. Stacy

*Department of Chemistry, University of California, Berkeley, California 94720*

T. Sands

*School of Materials Engineering, School of Electrical and Computer Engineering, Purdue University, West Lafayette, Indiana 47907*

M. A. Ryan and J. P. Fleurial

*Jet Propulsion Laboratory, California Institute of Technology, Pasadena, California 91109*

(Received 9 August 2004; accepted 25 October 2004)

Bismuth telluride nanowires are of interest for thermoelectric applications because of the predicted enhancement in the thermoelectric figure-of-merit in nanowire structures. In this letter, we carried out temperature-dependent thermal diffusivity characterization of a 40 nm diameter  $\text{Bi}_2\text{Te}_3$  nanowires/alumina nanocomposite. Measured thermal diffusivity of the composite decreases from  $9.2 \times 10^{-7} \text{ m}^2 \text{ s}^{-1}$  at 150 K to  $6.9 \times 10^{-7} \text{ m}^2 \text{ s}^{-1}$  at 300 K and is lower than thermal diffusivity of unfilled alumina templates. Effective medium calculations indicate that the thermal conductivity along nanowires axis is at least an order of magnitude lower than thermal conductivity of the bulk bismuth telluride. © 2004 American Institute of Physics. [DOI: 10.1063/1.1834991]

Recent developments in nanostructured thermoelectric materials show that highly efficient thermoelectric energy conversion could be forthcoming.<sup>1</sup> Among emerging nanostructures, thermoelectric nanowires receive considerable attention from researchers.<sup>2–5</sup> Bismuth telluride ( $\text{Bi}_2\text{Te}_3$ ) nanowires are particularly interesting because bulk  $\text{Bi}_2\text{Te}_3$  is the most efficient of materials used in thermoelectric applications near room temperature. They are also appealing for device applications because can be fabricated inexpensively through electrochemical deposition in nanochanneled alumina templates.<sup>6–9</sup> The templates are also perceived to serve as structural support for the fragile nanowires.<sup>10</sup> However, heat leakage through the anodic alumina layer may affect the overall thermoelectric efficiency. Knowledge of the thermal transport in  $\text{Bi}_2\text{Te}_3$  nanowires/alumina nanocomposite is essential for device applications. The thermal properties of the nanocomposite can be also used to gain insight into the thermal properties of embedded nanowires. Thermal conductivity measurements using the  $3\omega$  method<sup>11,12</sup> have been reported for Si nanowires embedded in a polymer matrix.<sup>13</sup>

This letter reports experimental thermal properties of a 40 nm  $\text{Bi}_2\text{Te}_3$  nanowires/alumina nanocomposite over the temperature range between 150 K and 300 K. The nanocomposite consists of porous anodic alumina of 30% porosity with highly ordered parallel cylindrical pores of 40 nm di-

ameter filled with  $\text{Bi}_2\text{Te}_3$  in proportion better than 95% through electrodeposition. Temperature-dependent thermal diffusivity characterization was carried out with a photothermoelectric technique, described briefly in the following section. The magnitude of the thermal conductivity reduction in 40 nm  $\text{Bi}_2\text{Te}_3$  nanowires in the direction parallel to the wire axis is assessed from the measured thermal diffusivity using an effective medium model.

Temperature-dependent thermal diffusivity characterization of a 40 nm  $\text{Bi}_2\text{Te}_3$  alumina nanocomposite has been carried out with a photothermoelectric technique.<sup>14,15</sup> The experimental setup is schematically represented in Fig. 1. In this method ac optical heating was applied to the front side of the sample and the temperature rise was detected at the

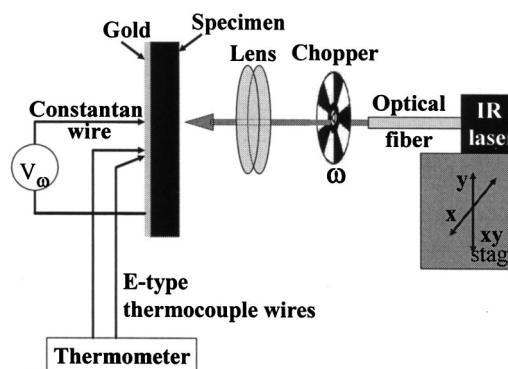


FIG. 1. Experimental setup for photothermoelectric technique. The local dc temperature rise of the sample is monitored using a pair of closely spaced E-type thermocouple wires. The sample is mounted in vacuum cryostat with optical access windows.

<sup>a)</sup> Author to whom correspondence should be addressed; electronic mail: gchen2@mit.edu

<sup>b)</sup> Current address: Department of Chemistry and Chemical Biology, Harvard University, Cambridge, MA 02138.

<sup>c)</sup> Current address: Instituto de Microelectrónica de Madrid, IMM (CNM-CSIC), C/Isaac Newton, 8 (PTM) 28760-Tres Cantos. Madrid, Spain.

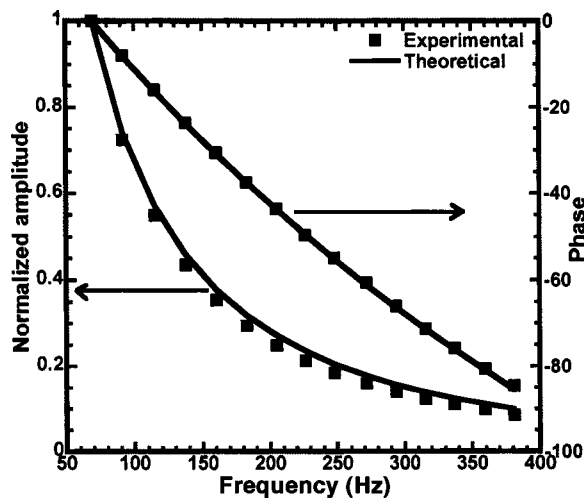


FIG. 2. Experimental (squares) and theoretical (lines) normalized amplitude and phase of the temperature rise. The fitting is carried out for phase of the thermal signal. Theoretical amplitude is calculated based on thermal diffusivity found fitting the phase.

backside. The ac heating on the front side was produced by a modulated IR laser beam with a diameter of  $\sim 0.75$  mm. The specimen thickness was  $64 \mu\text{m}$ . A thermocouple junction was formed between the backside of the sample and the tip of a constantan wire with a diameter of  $12.5 \mu\text{m}$ . Since the surface was nonconductive (the sample was polished to remove excess  $\text{Bi}_2\text{Te}_3$  prior to the experiment), a 50 nm gold layer was sputtered on the backside of the specimen to facilitate the temperature measurement. The amplitude and phase of the voltage generated by the thermocouple junction were measured using a lock-in amplifier.

The experimental data were initially fitted with a one-dimensional heat conduction model because the beam diameter was much larger than the sample thickness and it was assumed that the heat transfer occurred mainly across the specimen with very little spreading in the parallel direction. We also tried a two-dimensional anisotropic heat conduction model in cylindrical coordinates and we found that the fitted thermal diffusivity increased by 6%, hence these values are reported here. In the two-dimensional heat conduction model the heat capacity of the specimen was estimated from effective medium theory, based on the heat capacity of alumina templates<sup>16</sup> and the specific heat<sup>17</sup> and density<sup>18</sup> of  $\text{Bi}_2\text{Te}_3$ . The anisotropy of the thermal conductivity of the specimen was estimated from Maxwell's theory<sup>19</sup> for the limiting cases when  $\text{Bi}_2\text{Te}_3$  nanowires have negligible thermal conductivity (anisotropy  $\sim 0.76$ ) or the same thermal conductivity as bulk  $\text{Bi}_2\text{Te}_3$ <sup>20</sup> (anisotropy  $\sim 1$ ). The uncertainty in reported thermal diffusivity is  $\sim 9\%$  and it comes from uncertainty in sample thickness, which is  $\sim 4\%$ .

Figure 2 shows an example of the experimental temperature amplitude and phase, as compared with predictions using fitted values for thermal diffusivity. The fitting was carried out only for the phase of the thermal signal. Figure 3 shows the temperature dependent thermal diffusivity of the nanocomposite. The thermal diffusivity measured along the wires axis decreases from  $9.2 \times 10^{-7} \text{ m}^2 \text{ s}^{-1}$  at 150 K to  $6.9 \times 10^{-7} \text{ m}^2 \text{ s}^{-1}$  at 300 K. The room temperature thermal diffusivity is the same as reported elsewhere on a similar specimen.<sup>21</sup> The measured thermal diffusivity of the nano-

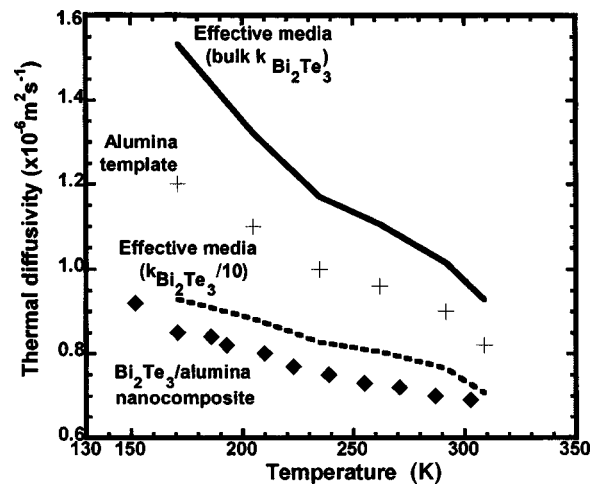


FIG. 3. Measured thermal diffusivity of 40 nm  $\text{Bi}_2\text{Te}_3$ /alumina nanocomposite (diamonds) and unfilled alumina template of similar porosity ( $\sim 30\%$ ). For comparison predictions of Eq. (1) are also shown when  $\text{Bi}_2\text{Te}_3$  nanowires have a thermal conductivity same as bulk (continuous line) or reduced by 10 times (dashed line).

composite is lower than the thermal diffusivity of unfilled alumina templates.

In order to assess the thermal conductivity reduction of the embedded BiTe nanowires, the experimental data are compared against predictions based on the effective medium theory. In this model, the thermal diffusivity ( $\alpha$ ) of the  $\text{Bi}_2\text{Te}_3$ /alumina nanocomposite along the nanowire axis is calculated as:

$$\alpha = \frac{k_{\text{alumina}} \cdot (1 - \phi) + k_{\text{Bi}_2\text{Te}_3} \cdot \phi}{(\rho c)_{\text{alumina}} \cdot (1 - \phi) + (\rho c)_{\text{Bi}_2\text{Te}_3} \cdot \phi}, \quad (1)$$

where  $k$  and  $(\rho c)$  represent the thermal conductivity and heat capacity of alumina and  $\text{Bi}_2\text{Te}_3$ , respectively, and  $\phi$  is the percentage of  $\text{Bi}_2\text{Te}_3$  in the composite. Assuming the nanowire properties are the same as those of bulk  $\text{Bi}_2\text{Te}_3$ , the calculated values significantly overpredict the results. If the nanowires have thermal conductivity at least an order of magnitude smaller than the bulk, the predicted values are close to the measured thermal diffusivity, within the upper limit of experimental errors. However predictions of Eq. (1) fit better the measured values if the thermal conductivity of  $\text{Bi}_2\text{Te}_3$  nanowires is reduced 30 times or more. An order of magnitude reduction in thermal conductivity was reported for individual 391 nm  $\text{Bi}_2\text{Te}_3$  nanowires grown by the same electrodeposition method.<sup>22</sup> However the diameter of the nanowires in the nanocomposite measured in the present study is ten times smaller and a larger thermal conductivity reduction is expected in these wires because of stronger size effects on heat carriers. Despite the estimated large thermal conductivity reduction in  $\text{Bi}_2\text{Te}_3$  nanowires we should point out that the good thermal properties of alumina template and the large uncertainties in the thermal diffusivity values of the nanowire-filled template make an exact determination of the thermal conductivity value of the nanowires impracticable.

In summary, we have measured the temperature-dependent thermal diffusivity of a 40 nm  $\text{Bi}_2\text{Te}_3$ /alumina nanocomposite. The alumina templates of 30% porosity and 40 nm diameter parallel pores have been filled with  $\text{Bi}_2\text{Te}_3$  through electrochemical deposition. The measured thermal diffusivity of the nanocomposite decreases from  $9.2$

$\times 10^{-7} \text{ m}^2 \text{ s}^{-1}$  at 150 K to  $6.9 \times 10^{-7} \text{ m}^2 \text{ s}^{-1}$  at 300 K. These values are lower than the thermal diffusivity of unfilled alumina templates and indicate that thermal conductivity of  $\text{Bi}_2\text{Te}_3$  nanowires is reduced at least an order of magnitude from the bulk value. This suggests that the thermal conductivity reduction in nanowires can be exploited for enhancing the thermoelectric figure of merit. However, the fact that the thermal conductivity of the templates overwhelms that of the composites also points out the need to develop alternative templates.

G.C. would like to acknowledge financial support from JPL and DOE. M.S.M.G. acknowledges a fellowship awarded by the MCYT (Spain) in the Ramon y Cajal Program.

<sup>1</sup>G. Chen, M. S. Dresselhaus, G. Dresselhaus, J.-P. Fleurial, and T. Caillat, *Int. Mater. Rev.* **48**, 45 (2003).

<sup>2</sup>X. Sun and M. S. Dresselhaus, *Appl. Phys. Lett.* **74**, 4005 (1999).

<sup>3</sup>J. Heremans, C. M. Thrush, Y.-M. Lin, S. Cronin, Z. Zhang, M. S. Dresselhaus, and J. F. Mansfield, *Phys. Rev. B* **61**, 2921 (2000).

<sup>4</sup>Y.-M. Lin, O. Rabin, S. B. Cronin, J. Y. Ying, and M. S. Dresselhaus, *Appl. Phys. Lett.* **81**, 2403 (2002).

<sup>5</sup>O. Rabin, Y.-M. Lin, and M. S. Dresselhaus, *Appl. Phys. Lett.* **79**, 81 (2001).

<sup>6</sup>A. L. Prieto, M. S. Sander, M. S. Martín-González, R. Gronsky, T. Sands, and A. M. Stacy, *J. Am. Chem. Soc.* **123**, 7160 (2001).

<sup>7</sup>J.-P. Fleurial, J. A. Herman, G. J. Snyder, M. A. Ryan, A. Borshchevsky, and C.-K. Huang, *Mater. Res. Soc. Symp. Proc.* **626**, Z11.3.1 (2000).

<sup>8</sup>M. S. Martín-González, G. J. Snyder, A. L. Prieto, R. Gronsky, T. Sands, and A. M. Stacy, *Nano Lett.* **3**, 973 (2003).

<sup>9</sup>M. S. Martín-González, A. L. Prieto, R. Gronsky, T. Sands, and A. M. Stacy, *Adv. Mater. (Weinheim, Ger.)* **15**, 2003 (2003).

<sup>10</sup>M. A. Ryan and J. P. Fleurial, *Electrochem. Soc. Interface* **11**, 30 (2002).

<sup>11</sup>D. G. Cahill and R. O. Pohl, *Phys. Rev. B* **35**, 4067 (1987).

<sup>12</sup>T. Borca-Tasciuc, A. R. Kumar, and G. Chen, *Rev. Sci. Instrum.* **72**, 2139 (2001).

<sup>13</sup>A. R. Abramson, W. C. Kim, S. T. Huxtable, H. Y., Y. Wu, A. Majumdar, C.-L. Tien, and P. Yang, *J. Microelectromech. Syst.* **13**, 505 (2004).

<sup>14</sup>D.-A. Borca-Tasciuc, G. Chen, Y.-M. Lin, O. Rabin, M. S. Dresselhaus, A. Borshchevsky, J.-P. Fleurial, and M. Ryan, *Mater. Res. Soc. Symp. Proc.* **703**, V2.7.1 (2001).

<sup>15</sup>T. Borca-Tasciuc, D.-A. Borca-Tasciuc, and G. Chen (unpublished).

<sup>16</sup>D.-A. Borca-Tasciuc and G. Chen (unpublished).

<sup>17</sup>Y. S. Touloukian, R. W. Powell, C. Y. Ho, and M. C. Nicolau, *Thermophysical Properties of Matter, Specific Heat: Nonmetallic Solids* (IFI/Plenum, New York, 1970).

<sup>18</sup>Material Safety Data Sheet, Alfa Aesar®, Ward Hill, MA 01835.

<sup>19</sup>J. C. Maxwell, *A Treatise on Electricity and Magnetism*, 2nd ed. (Clarendon, Oxford, 1881).

<sup>20</sup>D. M. Rowe, *CRC Handbook of Thermoelectrics* (CRC, Boca Raton, FL, 1995).

<sup>21</sup>D. Borca-Tasciuc, G. Chen, M. S. Martín-González, A. L. Prieto, A. Stacy, and T. Sands, *Proceedings of International Mechanical Engineering Congress and Exhibitions (IMECE2002)*, New Orleans, LA, 17–22 November 2002, paper No. IMECE2002-32774.

<sup>22</sup>D. Li, A. Prieto, Y. Wu, M. S. Martín-González, A. Stacy, T. Sands, R. Gronsky, P. Yang, and A. Majumdar, *The 21st International Conference on Thermoelectrics: ICT Symposia Proceedings*, Long Beach, CA, 25–29 August 2002, p. 333.